Eur Biophys J (2002) 31: 36–51
DOI 10.1007/s00249-001-0202-2

ARTICLE

**Nectarios Klonis · Melanie Rug · Ian Harper**
**Mark Wickham · Alan Cowman · Leann Tilley**

# Fluorescence photobleaching analysis for the study of cellular dynamics

Received: 19 July 2001 / Revised: 29 November 2001 / Accepted: 29 November 2001 / Published online: 1 February 2002


**Abstract** The wide availability of the confocal microscope and the emergence of green fluorescent protein (GFP) transfection technology has led to the increasing use of photobleaching studies to examine aspects of cellular dynamics in living cells. In this review, we examine the theory and practice of performing photobleaching studies using a confocal microscope. We illustrate the application of photobleaching protocols using our own measurements of fluorescently labelled red blood cells and of malaria parasite-infected erythrocytes expressing GFP fusions and examine other examples from the literature.

**Keywords** Green fluorescent protein · Fluorescence photobleaching · Fluorescence recovery after photobleaching · Confocal microscopy · Cell dynamics

**Abbreviations** *AOTF*: acousto-optical tunable filter · *CF*: carboxyfluorescein · *CLSM*: confocal laser scanning microscope · *DIC*: differential interference contrast · *FLIP*: fluorescence loss in photobleaching · *FRAP*: fluorescence recovery after photobleaching · *GFP*: green fluorescent protein · *PV*: parasitophorous vacuole

N. Klonis · M. Rug · L. Tilley (✉)
Department of Biochemistry,
La Trobe University, Bundoora, 3083 Victoria, Australia
E-mail: l.tilley@latrobe.edu.au
Fax: +61-3-4792467

N. Klonis · L. Tilley
Co-operative Research Centre for Diagnostics,
La Trobe University, Bundoora, 3083 Victoria, Australia

I. Harper
Department of Biological Sciences,
Monash University, Clayton, 3800 Victoria, Australia

M. Wickham · A. Cowman
Infection and Immunity,
Walter and Eliza Hall Institute of Medical Research,
PO RMH, 3052 Victoria, Australia

## Introduction

The technique of fluorescence recovery after photobleaching (FRAP, also known as fluorescence photobleach recovery or microphotolysis) was developed over two decades ago to study the diffusive characteristics of biological molecules in living cells (Axelrod et al. 1976). The method relies on the ability to incorporate a fluorescent label into specific protein or lipid components. The classical approach to performing FRAP measurements utilizes an epi-fluorescence microscope to focus the excitation beam to a small spot (~1 μm) on a region of interest in the cell. This beam is used to both bleach the fluorescent molecules in the region of interest and, in an attenuated form, to monitor the fluorescence from the same region. In the most common application of the technique, the fluorescence increases after bleaching owing to the diffusion of unbleached molecules into the illuminated region, so that an analysis of the fluorescence recovery provides the diffusion coefficient of the fluorescent molecule. However, any process that leads to the recovery of fluorescence may be quantified and examined by this method (see reviews by Webb 1981; Elson 1985; Petersen and Elson 1986; Meyvis et al. 1999; Reits and Neefjes 2001).

Until recently, performing photobleaching experiments required a dedicated instrument. The introduction of the confocal laser scanning microscope (CLSM) has made the technique available to anyone who has access to such an instrument. The CLSM generates images by focusing the laser to a diffraction-limited point on a specimen and recording the emitted fluorescence intensity through a small pinhole located at the confocal position in front of the detection unit. An image is built up pixel-by-pixel by scanning the diffraction-limited point across the specimen and represents a thin optical section of the specimen due to the rejection of out-of-focus light by the pinhole. Many confocal microscopes possess acousto-optical tuneable filters (AOTF), which permit the rapid (microsecond to millisecond) attenuation

of the laser (Kao and Verkman 1996) and hence allow the rapid switching between a bleaching and sampling beam to perform FRAP-type measurements.

The ability to use the CLSM to selectively bleach regions within the cell, coupled with the ability to quantitatively monitor the fluorescence from individual compartments within the cell, makes it possible to use photobleaching studies to answer a range of biological questions. Moreover, the ability to tag proteins of interest at the gene level with the green fluorescent protein (GFP) makes it possible to selectively target the fluorescent fusion protein to specific compartments of the cell and to monitor the fluorescence in live cells during the course of the cell cycle. Transfection approaches have provided valuable insights into the complex organization and reorganization of cellular components in real time and can provide considerably more information in combination with photobleaching methods (see reviews by Storrie and Kreis 1996; White and Stelzer 1999; Lippincott-Schwartz et al. 2000).

The purpose of this paper is to review the theory and practice of performing photobleaching studies with a CLSM. We begin with an outline of the classical approach to FRAP measurement and analysis and consider the additional approaches possible using the CLSM. We describe a number of literature reports of FRAP applications and illustrate some aspects of the technique using our own data for human erythrocytes labelled with fluorescent probes and for malaria parasite-infected erythrocytes expressing GFP-fusion proteins.

## Materials and methods

### Confocal microscopy and photobleaching

Specimens were mounted on a glass slide and covered by a glass coverslip (0.17 mm thickness; Longman Scientific, Melbourne, Australia). All samples were imaged within 30 min at ambient temperature (maintained at 20 °C) using an upright Leica TCS NT laser scanning confocal microscope with a 100× planapochromatic oil immersion objective (1.4 NA). Excitation was with a 60 mW Kr/Ar laser. Erythrocytes were labelled in the actin component with rhodamine-phalloidin as described by Knowles et al. (1997). 5(6)-Carboxyfluorescein *N*-hydroxysuccinimide ester (Molecular Probes, Eugene, Ore., USA) was reacted with casein (Sigma) in 0.1 M $NaHCO_3$, purified by gel filtration chromatography, and trapped inside hypotonically lysed and resealed erythrocytes as described by Knowles et al. (1997). For the carboxyfluorescein and GFP probes, excitation was with the 488 nm line and the emitted light was detected through a fluorescein filter set. For the rhodamine probe, excitation was with the 488 and 568 nm lines of the laser and the emission was detected through a tetramethylrhodamine filter set. The gain on the photomultiplier was kept high and the laser power was adjusted using an AOTF to a level sufficient to minimize photobleaching of the sample during image acquisition and to maintain pixel values below saturation in regions of interest. Image sizes were 512×512 pixels. Other parameters such as pixel resolution, speed of image acquisition and pinhole size are detailed in the figure legends.

Photobleaching studies were performed using the time-lapse feature of the Leica TCS NT software. The laser was focused on a single point (representing a diffraction-limited point) defined on a pre-bleach image. The point was illuminated with the unattenuated laser for a specified time and post-bleach images were obtained immediately after the high-intensity illumination and at time intervals after bleaching. A typical sequence would involve multiple pre-bleach images to assess the degree of bleaching during image acquisition, and multiple post-bleach images at different time intervals to follow recovery.

## Theory and analysis for determination of diffusion coefficients

### Conventional spot photobleaching

Biological molecules undergo translational diffusion within the three-dimensional space of a cellular system. Axelrod et al. (1976) considered the special case for measuring the two-dimensional diffusion of membrane components within a bilayer based on the model of Saffman and Delbruck (1975), which assumes that membrane-bound molecules are confined to an infinite plane but undergo free lateral diffusion within this fluid plane. Measurements are performed by illuminating the sample with a perpendicular beam with a radius $\omega$ in the object plane on the cell surface, where $\omega$ is the $1/e^2$ Gaussian radius. The beam is used both to produce localized bleaching in the illuminated region and to monitor the fluorescence from the same region. For the bleach event, the power of the beam is increased $10^3$–$10^4$ times to induce photochemical destruction of the molecules in the illuminated region. This effectively creates a concentration gradient of unbleached fluorophores across the bleached area. For a system containing a single diffusible species, the fluorescence intensity, $F$, increases as a function of time, $t$, after the bleach pulse, owing to diffusion of molecules into the area probed by the beam. The fluorescence recovers according to:

$$\frac{F(t)}{F_p} = \sum_{n=0}^{\infty} \left[ \left( \frac{(-K)^n}{n!} \right) \left( \frac{1}{1 + n(1 + 2t/\tau_D)} \right) \right] \quad (1)$$

where $K$ is a parameter related to the degree of bleaching:

$$\frac{F_o}{F_p} = \frac{(1 - e^{-K})}{K} \quad (2)$$

and $F_p$ and $F_o$ are the fluorescence intensities prior to and immediately after the bleach event, respectively. The $\tau_D$ parameter is the characteristic time of recovery and is related to both the beam radius and the diffusion coefficient ($D$) of the probed molecule:

$$\tau_D = \frac{\omega^2}{4D} \quad (3)$$

A common observation in FRAP measurements is that the fluorescence does not recover to its initial pre-bleach intensity owing to the presence of a population of fluorophores that is immobile on the time scale of the FRAP measurement (this will be discussed below).

Under these conditions, the recovery is described by (Tsuji and Ohnishi 1986):

$$\frac{F(t)}{F_p} = \alpha \sum_{n=0}^{\infty} \left[ \left( \frac{(-K)^n}{n!} \right) \left( \frac{1}{1+n(1+2t/\tau_D)} \right) \right] + (1-\alpha)\frac{F_o}{F_p} \tag{4}$$

where $\alpha$ represents the fraction of the mobile species:

$$\alpha = \frac{F_\infty - F_o}{F_p - F_o} \tag{5}$$

and $F_\infty$ is the fluorescence at infinite time. A simulation of a FRAP recovery curve generated according to Eq. (4) is shown in Fig. 1.

Equations (1) or (4) can be directly fitted to experimental FRAP data. However, the complex nature of these equations has led to alternative methods for extracting the relevant parameters from a FRAP curve. A common approach is to determine the half time of recovery ($\tau_{1/2}$) from a recovery curve (Axelrod et al. 1976). As shown in Fig. 1, $\tau_{1/2}$ is similar to $\tau_D$. The two values are related according to:

$$\tau_{1/2} = \beta\tau_D = \beta\frac{\omega^2}{4D} \tag{6}$$

where $\beta$ is a function of the degree of bleaching (1.22 in the example shown in Fig. 1; see Yguerabide et al. 1982). Since measuring the beam width is not a trivial matter (see below), the value of $\tau_{1/2}$ is often used and is considered sufficient to compare the relative diffusion coefficients of molecules, provided the beam width is kept constant (e.g. see McCown et al. 1981).

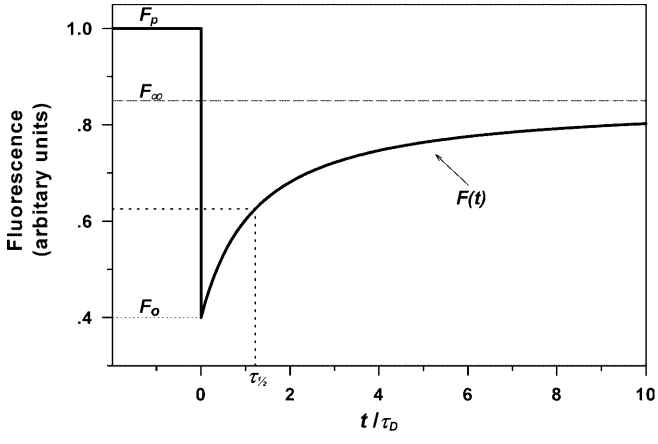


**Fig. 1** A simulated recovery curve illustrating relevant parameters of a FRAP experiment. At $t=0$ a high-intensity light beam is applied to a region on a fluorescently labelled cell, causing a rapid drop in the fluorescence signal. Owing to diffusional events, bleached molecules in this region exchange with unbleached molecules from other regions of the cell, allowing recovery of the fluorescence signal. In the case depicted, the final fluorescence intensity, $F_\infty$, is less than $F_p$ because a proportion of the fluorescent molecules are immobile on the time-scale of the experiment. $\tau_D$ is the characteristic time of recovery and is related to both the beam radius and the diffusion coefficient of the probed molecule. Data were simulated according to Eq. (4) with parameters $F_p=1$, $K=2.2$ (60% bleach), 75% mobile fraction. Also shown is the half time of recovery ($\tau_{1/2}$) at $t/\tau_D=1.22$

Other methods have been developed to analyse the data in a FRAP recovery curve and to identify whether convective flow or multiple diffusing species also contribute to the recovery. Yguerabide et al. (1982) and van Zoelen et al. (1983) have described methods for linearizing FRAP data which conform to Eq. (4). Kwon et al. (1994) have presented a useful empirical equation that can be directly fitted to FRAP data:

$$F(t) = F_o + \frac{(F_\infty - F_o)t}{t+\tau_{1/2}} \tag{7}$$

## Spot photobleaching using the CLSM

FRAP measurements can be performed and analysed as described above using the CLSM by parking the laser beam over the region of interest, bleaching with the unattenuated laser and then monitoring the fluorescence over the same region with the attenuated laser using an open pinhole. Considerably more information can be obtained by considering what happens to the fluorescence from regions of the cell that are not directly interrogated by the bleaching beam. Koppel (1979) described a way of doing this using multipoint scanning following either a spot or line bleach. Video and confocal microscopy permit recovery to be monitored over images of whole cells. The theoretical treatment of Axelrod et al. (1976) has been extended by Blonk et al. (1993)[1] to cover the time-dependence of the spatial distribution of fluorescence in images obtained with a fully open confocal aperture:

$$\frac{F(r,t)}{F_p} = \sum_{n=0}^{\infty} \left[ \frac{(-K)^n}{n!} \left( \frac{\exp\left(\frac{-2nr^2}{\omega^2\beta_n}\right)}{\beta_n} \right) \right] \tag{8}$$

where:

$$\beta_n = 1 + n\left(1 + \frac{2t}{\tau_D}\right) \tag{9}$$

and $r$ is the radial distance from the centre of the bleach spot. Figure 2 shows data simulations calculated using Eq. (8). The bleached area immediately after the bleach pulse appears to be broader than the beam profile (Fig. 2a) because the fluorescence image of the bleached region is a convolution of the actual image with the point spread function of the microscope. As a result, $\omega$

[1]Blonk et al. (1993) provide an equation which describes the spatial distribution of fluorescence in three dimensions following bleaching by a Gaussian beam, as would be measured in a CLSM with an open pinhole. Brown et al. (1999) argue that the equation is not valid for three-dimensional diffusion. However, this equation remains valid for the case considered here, i.e. two-dimensional diffusion within a membrane bilayer or for diffusion of a solute in the cytoplasm or in solution where the bleaching beam is effectively cylindrical

cannot be determined directly from the image without deconvolution. However, as a rule of thumb, Blonk et al. suggest that dividing the measured Gaussian radius by a factor of 1.6 can be used to determine the actual value of $\omega$ from the initial post-bleach image. During the course of recovery, there is a broadening of the radial distribution of intensity and a decrease in its amplitude (Fig. 2a). In addition, the recovery profile is dependent on the region being examined, with some regions exhibiting an initial decrease in intensity (Fig. 2b).

Post-bleach images can be analysed in a number of ways to extract the diffusion coefficient. The images can be analysed in Fourier space to provide the diffusion coefficient without any knowledge of the beam profile or the microscope's point spread function (Cardullo et al. 1991; Tsay and Jacobson 1991; Berk et al. 1993). The temporal changes in the amplitude and width of the spatial distribution of fluorescence can also be employed to measure the diffusion coefficient (Cardullo et al. 1991).

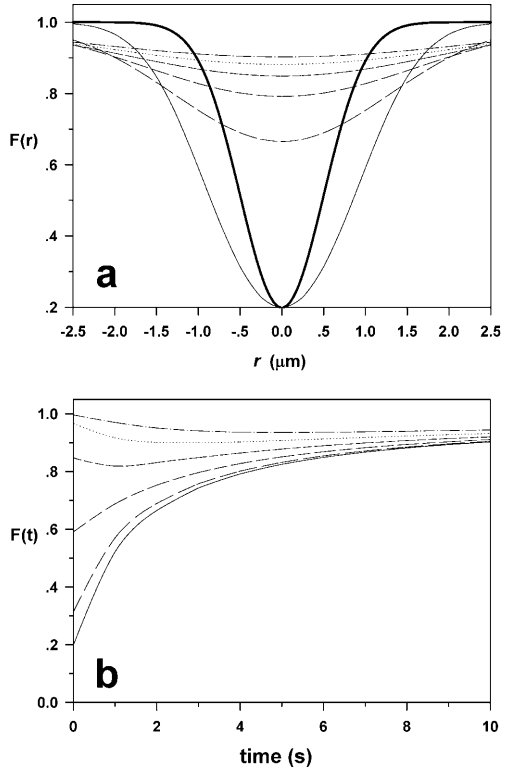


**Fig. 2a, b** Time-dependence of the radial distribution of fluorescence intensity in an illuminated region at different times following photobleaching with a Gaussian beam. **a** The fluorescence signal ($F$) is plotted as a function of $r$, the radial distance from the centre of the bleach spot. Data were simulated according to Eq. (8) with the following parameters: $\omega = 1$ μm; $D = 0.25$ μm$^2$/s; $\tau_D = 1$ s; $K = 5$. Shown in *thin lines from the lower to the upper curve* are the radial distributions at 0, 2, 4, 6, 8 and 10 s after bleaching. Also shown is a Gaussian profile with $\omega = 1$ μm (*thick line*), which represents the profile of the bleaching beam and hence the initial concentration gradient of fluorophores at time 0. **b** Curves *from bottom to top* represent the recovery of fluorescence following photobleaching calculated from the data in **a** at radial positions of 0, 0.5, 1, 1.5, 2 and 2.5 μm plotted as a function of time after photobleaching

In principle, the intensity of the pixel at the centre of the bleached region can be analysed using the approaches described above for conventional spot photobleaching. In practice, we have found that individual pixel values are too noisy in real data obtained from a confocal image to be analysed in this way. Considerable improvement in signal-to-noise can be obtained by using the average pixel value in the region of the bleach centre. This approach is valid provided the region examined is less than the width of the bleaching beam (Blonk et al. 1993; Wedekind et al. 1996). As shown in the simulated data in Fig. 3a, the recovery profile is altered when values are averaged over larger areas and in some cases the recovery curve is sigmoidal. The recovery of the average fluorescence intensity within a circle of radius $w_r$

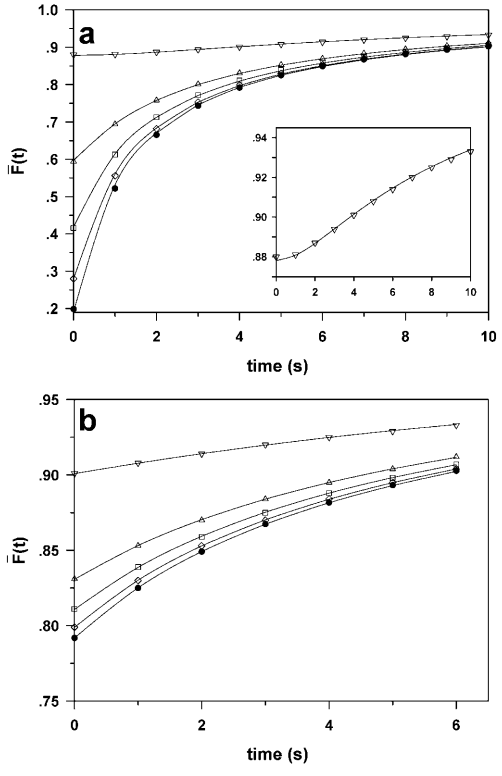


**Fig. 3a, b** Analysis of the recovery of the fluorescence signal within an illuminated region following bleaching by a Gaussian beam. **a** The average fluorescence intensity is followed as a function of time for data simulated on a two-dimensional pixel grid using the same parameters as in the previous figure. The average intensity within a radius ($w_r$) of 0.6 (*diamonds*), 1 (*squares*), 1.5 (*up triangles*) and 3 μm (*down triangles*) of the bleach centre are shown at different times following the bleach. Also shown is the fluorescence of the pixel at the bleach centre (*solid circles*). *Inset*: expanded plot of data at 3 μm. The curves are the results of non-linear regression analysis using Eq. (10). The value of $w$ was fixed at 1.67 μm, based on fitting of the $t = 0$ curve in Fig. 2a to a Gaussian distribution. The $F_o$, $F_\infty$ and $D$ values were floated and the data analysed globally using the same mobile fraction ($\alpha$) and $D$ value to link each data set. The fitted $\alpha$ and $D$ values are 1.00 and 0.255 μm$^2$/s, respectively. **b** The same data as in **a** but with the 4 s time point reset to zero time. The analysis was performed in the same way but with the $w$ value (3.25 μm) obtained from the $t = 4$ s curve in Fig. 2a. The fitted parameters were $\alpha = 1.00$ and $D = 0.253$ μm$^2$/s

of the bleach centre can be calculated according to Berk et al. (1993):

$$\bar{F}(t) = \bar{F}_{\mathrm{p}} - \left(\frac{1 - \exp\left(-2\gamma^2/\left(1 + 8Dt/w^2\right)\right)}{1 - \exp(-2\gamma^2)}\right)\left(\bar{F}_{\mathrm{p}} - \bar{F}_{\mathrm{o}}\right) \quad (10)$$

where:

$$\gamma = \frac{w_{\mathrm{r}}}{w} \quad (11)$$

and $w$ is the Gaussian radius of the bleaching beam and the horizontal bar over the parameters denotes that they represent the average values calculated within a circle of radius $w_{\mathrm{r}}$ of the bleach centre. In the formulation of Berk et al. (1993), $w$ is equivalent to $\omega$ and the fluorescence intensity at each position in the image is directly proportional to the concentration of fluorescent molecules at that position. Hence, Eq. (10) is valid for situations where $w$ or $\omega$ is much greater than the diffraction limit but cannot strictly be employed when employing $\omega$ at the diffraction limit, since the fluorescence intensity is a function of the fluorescence intensity in the region and the microscope point spread function. However, as shown in Fig. 3a, we have found that simulated data can be accurately analysed using Eq. (10) if the value of $w$ used is the Gaussian radius of the fluorescence distribution (1.67 μm) rather than the actual beam radius (1 μm). Moreover, the data can also be successfully analysed even if the initial time points of the recovery phase are missed. For example, Fig. 3b shows the same data as in Fig. 3a but with the data at time $t = 4$ s set to zero time. The correct diffusion coefficient is obtained if the Gaussian radius of the new $t = 0$ image (3.25 μm) is employed. These results indicate that this analytical approach does not require knowledge of the actual beam width or the acquisition of the initial image immediately after the bleach pulse. As such, it may be valid for the analysis of a single diffusing species (or a single diffusing species in the presence of an immobile population) in any situation where the radial distribution of fluorescence is Gaussian in nature.

### Additional photobleaching formats using the CLSM

The FRAP technique can be carried out using a number of different photobleaching formats. These include (1) bleaching with a uniform disc illumination or line profile (Koppel 1979; Soumpasis 1983), (2) the pattern photobleaching or modulation method (Smith and McConnell 1978; Mozo-Villarias and Ware 1985), (3) continuous scanning microphotolysis (Peters et al. 1981), (4) polarized photobleaching (Smith et al. 1981; Velez and Axelrod 1988; Scalettar et al. 1990) and (5) in association with total internal reflection microscopy (Thompson et al. 1993). The flexibility of the confocal microscope means that it can be employed using additional bleaching formats. For example, rectangular bleaching profiles can be obtained by zooming in on the area to be bleached, imaging the area using an unattenuated laser, then zooming out and imaging the fluorescence recovery with an attenuated laser. Line bleaches can be employed in a similar way by using the $xt$ scanning function of the microscope. The more recent commercially available confocal microscopes permit the user to define and bleach regions of interest in almost any pattern or shape. Kubitscheck et al. (1994) describe a variance method for analysing fluorescence recovery following bleaching using radially symmetric profiles. This analysis has been demonstrated for both uniform disc (Kubitschek et al. 1994) and for rectangular (Gribbon and Hardingham 1998) bleaching profiles. Wedekind et al. (1996) describe the use and analysis of variable line bleaching using line scanning, the major advantage of which is the increased temporal resolution for measuring fast diffusive processes.

## Considerations and problems in FRAP analysis

### General aspects

#### *Degree of bleaching (K parameter)*

The degree of bleaching needs to be $< 80\%$ ($K < 5$) for the proper analysis of conventional spot photobleaching data. Bleaching levels greater than this result in a non-Gaussian distribution of molecules following bleaching (see Axelrod et al. 1976).

#### *Bleach times and recovery times*

The accurate analysis of FRAP data requires that the bleach event is essentially instantaneous. In practice, this means that it must be much shorter than the recovery time. In addition, the accurate quantification of the immobile population requires the recovery event to be monitored for times much greater than $\tau_{1/2}$ or $\tau_{\mathrm{D}}$ (see Fig. 1).

It is instructive to consider recovery times for different molecules using a typical beam radius of 1 μm. Membrane-embedded proteins in cells typically exhibit $D$ values of 0.001–0.01 $\mu m^2/s$, corresponding to $\tau_{\mathrm{D}}$ values in the hundreds of seconds. Hence, bleach times of 10–100 ms with recoveries monitored over tens of minutes are employed. In contrast, membrane phospholipids ($D \approx 0.1$–1 $\mu m^2/s$; $\tau_{\mathrm{D}} \approx 0.1$–1 s) require millisecond bleach times with recovery monitored over seconds. FRAP measurements of soluble molecules such as proteins ($D \approx 10$–100 $\mu m^2/s$; $\tau_{\mathrm{D}} \approx 0.001$–0.01 s) require specialized instrumentation which can produce microsecond bleach pulses and can rapidly switch to a sampling beam to monitor the millisecond recovery. Alternatively, since the recovery time is dependent on $\omega^2$, the beam radius

can be altered so that the recovery occurs on an appropriate time scale for measurement (see below). A point worth noting when altering bleach times is that the bleaching beam must possess a greater intensity for short bleach times in order to obtain the same degree of bleaching.

*Beam radius*

Knowledge of the beam profile ($\omega$) is necessary for the correct determination of the diffusion constant (Eq. 3). A number of methods have been described for directly measuring this parameter (e.g. see Zs.-Nagy et al. 1985; Stolpen et al. 1988). Alternatively, $\omega$ can be calculated from the recovery time of a standard possessing a known diffusion coefficient (Thompson and Axelrod 1980). Wolf et al. (1980a) have also suggested measuring the diffusion coefficients of standards to ensure that reports from different laboratories can be directly compared.

The beam radius can be varied to confirm that the recovery time obeys the expected dependence on $\omega^2$ in order to confirm that the recovery is due to diffusion (Wu et al. 1978). This can be achieved by changing the magnification/aperture of the objective or by focusing the beam above or below the area of interest to generate a larger bleach profile (Barisas and Leuther 1979; Yechiel and Edidin 1987).

*Relative geometry of sample and beam*

The fluorescence recovery described by Eqs. (4) and (10) assumes the diffusing molecule is located in an infinite plane perpendicular to the illuminating beam and that recovery occurs due to diffusion of the molecule in two dimensions. This is an adequate approximation for molecules confined to the plasma membranes of many cells. However, this is not valid for cells where the membrane geometry approximates a cylinder, for example in sperm flagella or neuronal processes (Wolf 1992), or for cells containing convoluted membranes, for example microvilli or blebs (Aizenbud and Gershon 1982). In these cases, other analytical approaches are required. For example, Wey et al. (1981) considered the situation where a Gaussian beam was used to bleach rhodopsin in rod outer-membrane segments. In this case the optical axis is parallel rather than perpendicular to the membranes and the fluorescence recovery is effectively due to one-dimensional diffusion. In addition, Wey et al. (1981) considered effects that arise due to a finite system (i.e. where a significant proportion of the total population of fluorescent molecules undergoes photodestruction).

Similarly, many intracellular organelles cannot be modelled as planar structures and the fluorescence recovery cannot be directly related to the diffusion coefficient of the molecular species using the above approaches. In their analysis of diffusion in the endoplasmic reticulum (ER) membrane, Sciaky et al. (1997) and Siggia et al. (2000) modelled the ER as a series of randomly orientated and connected tubular and cisternal components with a non-uniform spatial distribution. A large rectangular region of the ER was bleached and the entire pre-bleach and post-bleach images were used in the analysis so that the variation in density and geometry of the ER in the cell was taken into account. It was assumed that recovery occurred owing to a single one-dimensional diffusion coefficient and that the fluorescence recovered towards the pre-bleach intensity. In the special case where the fluorescence is totally bleached, the recovery of fluorescence within the bleached strip can be fitted to the empirical equation:

$$F(t) = F_\infty \left( 1 - \sqrt{\frac{w^2}{w^2 + 4\pi D_{1D} t}} \right) \tag{12}$$

where $D_{1D}$ is the one-dimensional diffusion coefficient and $w$ is the width of the bleached strip. According to Ellenberg et al. (1997), the recovered diffusion coefficient of a membrane component can be estimated within an accuracy of 30% with this equation.

Complications in the analysis of diffusion can also arise from the fact that the illuminating beam has a three-dimensional profile (i.e. it bleaches and records fluorescence in a three-dimensional volume). This is particularly a problem for the analysis of the diffusion of cytoplasmic components. The analysis can be simplified by using a low-power objective to produce a beam profile that is approximately cylindrical so that recovery is effectively due to two-dimensional diffusion (Wojcieszyn et al. 1981; Kreis et al. 1982). An alternative approach is to relate the half time of recovery to standards (Kao et al. 1993; Seksek et al. 1997).

A number of studies have demonstrated the feasibility of performing FRAP measurements to investigate diffusion of soluble components in the lumen of the mitochondria and ER (Olveczky and Verkman 1998; Partikian et al. 1998; Dayel et al. 1999). These structures were modelled as thin cylinders and planar sheets, respectively. It is found that such geometries have little effect on the recovery time compared to unrestricted diffusion in solution, even when the mitochondria contain significant occlusions.

*Photobleaching artefacts*

A number of studies have demonstrated the validity of results obtained with the FRAP technique (see White and Stelzer 1999). Initially it was suggested that local heating caused by the bleach pulse might artefactually increase the rate of diffusion of molecules close to the beam profile. However, Axelrod (1977) calculated that the temperature increase due to bleach illumination under typical conditions was 0.3 °C. Wolf et al. (1980b) labelled two different components in a cell membrane

and demonstrated that the bleaching of one component did not affect the recovery of the second component. Wey et al. (1981) demonstrated that the diffusion coefficient of rhodopsin measured by FRAP is the same as that determined with other techniques. Nonetheless, the intense illumination required to bleach fluorescent molecules can have a number of undesirable effects on the system being investigated (see Wolf et al. 1980b). For example, cross-linking of membrane proteins (Lepock et al. 1978), deleterious effects on microtubules (Takeda et al. 1995) and damage to erythrocytes (Bloom and Webb 1984) have been reported following exposure to intense radiation. Corbett et al. (1994) also reported that different results may be obtained under low and normal oxygen levels.

### *Reversible photobleaching*

Recent studies have shown that many of the common fluorophores utilized in FRAP are not irreversibly bleached but exhibit a small degree of reversibility on the microsecond and millisecond time scales. This effect has been shown for carboxyfluorescein under deoxygenated conditions (Stout and Axelrod 1995), fluorescein in viscous media (Periasamy et al. 1996) and wild-type GFP in viscous media (Swaminathan et al. 1997). This has important consequences for the analysis of FRAP data, especially for fast diffusive processes that recover on similar time scales (e.g. soluble proteins). A simple way of identifying whether reversible photobleaching is occurring is to bleach the entire cell and look for any fluorescence recovery.

## CLSM-specific considerations

### *Bleaching during image acquisition*

The intensity of the scanning laser employed in the acquisition of typical confocal images is often sufficient to produce significant bleaching of the sample during the course of image acquisition. In fact, each point in the scanned sample receives the same total intensity of light, resulting in an even bleaching of the whole sample. A number of approaches can be employed to reduce this background bleaching. These include (1) decreasing the pixel resolution by zooming out, (2) employing line scans rather than 2D scans, (3) decreasing pixel dwell times by using faster scans, (4) decreasing the laser power and (5) using fluorescent probes that are less susceptible to photobleaching. Obviously some of these approaches result in a decrease in the signal-to-noise ratio. This can be partly compensated by increasing the aperture of the confocal pinhole, but this comes at the expense of a decrease in resolution of the image.

Although undesirable, a small degree of background bleaching can be tolerated and corrected for. Because background bleaching is effectively constant throughout the field of view, the fluorescence intensities in a region of the cell that is far from the bleached region, or in another cell in the field of view, can be employed to correct the images for this effect. Alternatively, the data can be corrected by normalizing the total fluorescence intensity in each image (e.g. see Dundr et al. 2000).

### *Cell movement during image acquisition*

Small translations or morphology changes in cells can affect the quantitation of fluorescence during a bleach experiment. This is particularly important for measurements performed using a confocal pinhole with a small aperture, as even small movements can affect which part of the cell is in the image view. A convenient way of checking for such movement is to compare 8-bit fluorescence or differential interference contrast (DIC) images at different times (i.e. Image 1 and Image 2) using the following formula to generate a difference (DIFF) image:

$$\mathrm{DIFF} = \frac{(\mathrm{Image\ 1} - \mathrm{Image\ 2})}{2} + 128 \tag{13}$$

When DIFF is viewed as a greyscale image, regions where there is no difference between the two images appear grey, whereas regions with increased pixel values approach black and regions with decreased pixel values approach white. As a result, regions that have moved slightly between the images appear as reliefs; large-scale movements give rise to a white-and-black image of the region.

### *Time resolution*

The AOTF on a confocal microscope can typically switch between bleaching and sampling modes in milliseconds and acquisition of a 512×512 image typically requires ~1 s. These times are sufficiently rapid to allow accurate measurements of the diffusion rates of most membrane proteins using a spot bleach approach; however, they are not adequate for measuring faster diffusive processes. The speed of image acquisition can be increased ~5-fold by taking smaller images or using faster scans. A more than 100-fold increase in time resolution can be achieved by using a line scan rather than a 2D scan. This is sufficient to allow the analysis of the diffusion of membrane phospholipid and soluble proteins. The increased time resolution comes at the expense of signal quality and the number of pixels that can be utilized in the analysis.

An alternative approach for measuring fast diffusive process is to increase the effective recovery time by increasing the size of the bleached area. From Eq. (3), it follows that a bleach spot with a radius of 10 μm produces a recovery time on the order of seconds for a component with a diffusion coefficient on the order of 10 $\mu m^2/s$. Large bleaching profiles can thus permit accurate quantitation of soluble protein diffusion. Square

bleach profiles in this range can be performed on most available confocal microscopes using the zoom function.

*Pixel saturation*

Most confocal microscopes currently in use produce 8-bit images. For accurate quantitation of images it is necessary to adjust the power of the illuminating beam and/or the gain on the photomultiplier to limit the number of pixels that exhibit the maximum intensity (255). This may present a problem, particularly for noisy images since it means that the average pixel value may be substantially less than this maximum, thus effectively decreasing the dynamic range of the measurement. Thus features on the cell that differ in intensity by a factor of 10 are difficult to quantify in the same measurement. This problem can be partly alleviated by increasing the dwell time per pixel (i.e. using slower scans), but this comes at the price of increasing background bleaching and decreasing time resolution. Newer confocal microscopes offer the possibility of acquiring 12-bit images, which increases the dynamic range and alleviates many of these problems.

*Choice of fluorescent probes*

The ideal fluorescent probe for photobleaching studies is highly fluorescent and moderately susceptible to photobleaching. This permits bleaching within realistic time frames but limits bleaching during image acquisition. We have found that fluorescein is not the ideal probe for quantitative FRAP studies using the CLSM, owing to large background bleaching during image acquisition. The Alexa series of dyes appear to have superior properties in that they exhibit high fluorescence yields and relatively low susceptibility to bleaching during image analysis, but can be adequately bleached by a 0.1–1 s exposure to a full power laser illumination. Some GFP mutants also exhibit very good photostability characteristics (Patterson et al. 1997), which is an advantage for image acquisition, but require longer bleach times (e.g. $>1$ s) to achieve adequate bleaching.

## Applications to cell biology and variations on the basic technique

Diffusion in the plasma membrane

The earliest applications of FRAP examined the diffusion of plasma membrane proteins and phospholipids (see reviews by Axelrod 1983; Peters 1983; Jacobson et al. 1987; Jovin and Vaz 1989; Tocanne et al. 1989). The diffusion of small molecules, such as phospholipids, that are comparable to the size of the molecules that make up the membrane bilayer can be modelled by free volume theory (Vaz et al. 1984). Membrane phospholipids typically exhibit diffusion coefficients close to these predicted values (0.1–1 $\mu m^2/s$) and the mobile population is usually close to 100% (Vaz et al. 1985).

The diffusion coefficients of large molecules such as proteins can be predicted on the basis of the model of Saffman and Delbruck (1975), which treats membrane-embedded components as cylinders diffusing in a medium of uniform viscosity. The model predicts that the diffusion coefficient is only weakly dependent on the radius of the diffusing species. Thus the diffusion rate of a membrane protein is expected to be only a few-fold slower than that of phospholipids. The diffusion rates of some membrane proteins are well predicted by the Saffman/Delbruck model. For example, proteins, such as rhodopsin and the Thy1 antigen (which is associated with the membrane via a lipid anchor), and a number of membrane proteins that have been reconstituted into synthetic vesicles, have been shown to diffuse with close to expected diffusion rates (Cone 1972; Poo and Cone 1974; Peters and Cherry 1982; Ishihara et al. 1987). However, most membrane proteins in cells exhibit diffusion coefficients (0.001–0.01 $\mu m^2/s$) that are 10–100 times lower than expected values and a significant proportion of the population may be immobile on the time scale of the FRAP measurements (Vaz et al. 1982; Yechiel and Edidin 1987; Tocanne et al. 1989). This has been generally attributed to interactions of membrane proteins with other proteins and/or the underlying cytoskeleton (e.g. Edidin et al. 1994).

More recent measurements of membrane protein diffusion utilizing single particle tracking or ''optical tweezers'' methods have revealed that the diffusion of individual molecules is not isotropic. Rather, the molecules appear to be temporarily restricted to microscopic domains before diffusing to adjacent domains. A number of models that take this into account have been developed (Jacobson et al. 1995; Feder et al. 1996; Cherry et al. 1998; Periasamy and Verkman 1998; Salome et al. 1998). An interesting conclusion is that the incomplete recovery observed in many FRAP measurements may represent the spatial and temporal dependence of diffusion due to these submicroscopic heterogeneities in the membrane rather than two distinct populations of molecules.

In many cells the heterogeneity of the plasma membrane is clearly evident on the macroscopic scale. For example, Angelides et al. (1988) found that voltage-dependent sodium channels, which are non-uniformly distributed in nerve cells, show rapid diffusion ($D \approx 0.1$ $\mu m^2/s$) in the cell body and slower ($D \approx 0.001$–$0.01$ $\mu m^2/s$) diffusion in the axon hillock. Thomas et al. (1994) found that the phospholipid probe 3,3′-dihexadecylindocarbocyanine, which tends to co-aggregate with immunoglobulin E receptors in rat basophilic leukaemia cells, is immobile in the aggregated regions but mobile in the other regions. Cowan et al. (1997) found that a number of membrane proteins were confined to specific domains in the plasma membrane of guinea pig sperm but exhibited free diffusion within these domains,

indicating, in this case, the presence of barriers located at the domain boundaries.

## Diffusion in intracellular membranes

Investigations of the dynamics of lipids and proteins in intracellular organelles are comparatively recent. In contrast to most plasma membrane proteins, most membrane-embedded proteins in the ER and Golgi that have been examined exhibit large mobile fractions and diffusion coefficients, similar to those expected from the Saffman and Delbruck model, i.e. $D = 0.1–0.5\ \mu m^2/s$ (Storrie et al. 1994; Cole et al. 1996; Ellenberg et al. 1997; Sciaky et al. 1997; Nehls et al. 2000). Cytochrome P450 is an exception, exhibiting a diffusion coefficient that is ten times lower ($D = 0.06\ \mu m^2/s$; Szczesna-Skorupa et al. 1998). Sciaky et al. (1997) have also found that the rate at which Golgi contents are resorbed into the ER during brefeldin A treatment cannot be explained by simple membrane diffusion and suggest that the transport in this case occurs via flow-assisted membrane transport processes.

The rate of diffusion of emerin-GFP in the inner nuclear membrane has been reported to be similar to that in the ER and Golgi membranes (Ostlund et al. 1999). By contrast, the lamin B receptor and POM121, which forms part of the nuclear pore complex, are essentially immobile (Ellenberg et al. 1997; Daigle et al. 2001). However, in both cases the proteins are highly mobile when the nuclear envelope is absorbed into the ER during mitosis.

## Diffusion in the cytoplasm and in the lumen of intracellular organelles

The diffusion coefficient of a solute is related to the viscosity of the medium and the size of the molecule according to the Stokes-Einstein equation. For a protein in solution this corresponds to $D \approx 10–100\ \mu m^2/s$. FRAP measurements using macromolecules that do not interact with other cytoplasmic elements have revealed that diffusion in the cytoplasm is 3- to 4-fold slower than in water (Luby-Phelps et al. 1986, 1987; Kao et al. 1993; Seksek et al. 1997; Swaminathan et al. 1997; Arrio-Dupont et al. 2000). This decrease has been attributed to the increased viscosity of the cytoplasm and/or the presence of elements that create a cytoplasmic meshwork, which acts as a barrier and restricts diffusion. Some studies have concluded that molecules much larger than 26 nm (Luby-Phelps et al. 1986, 1987) exhibit severe restriction in their diffusion, although other studies dispute this (Seksek et al. 1997). However, the latter studies also report an increase in the immobile fraction for molecules with increased size.

Early FRAP measurements of diffusion coefficients of components in the cytoplasm yielded values of about $1\ \mu m^2/s$, which were independent of the size of the protein (Wojcieszyn et al. 1981; Jacobson and Wojcieszyn 1984). This was attributed to the interaction of the proteins with cytoplasmic elements. Other studies have also shown that some cytoplasmic proteins have much lower diffusion rates. For example, Luby-Phelps et al. (1995) found that 95% of the calmodulin in smooth muscle cells was immobile and the remainder possessed a 7-fold lower diffusion coefficient compared to a dextran of equivalent size. This indicates that the calmodulin is not present as a freely diffusible species but is compartmentalized in the cytoplasm. Swaminathan et al. (1996) found that the diffusion of a small fluorescent molecule was 6- to 10-fold slower in cytoplasmic regions close to the plasma membrane, perhaps reflecting increasing meshing of cytoskeletal elements in this region. Much larger effects have been observed in the periplasm of *Escherichia coli*, where diffusion coefficients of soluble proteins were found to be 1000-fold lower than in water (Brass et al. 1986).

Partikian et al. (1998) found that the rate of diffusion of a GFP fusion protein in the mitochondrial lumen was similar to that in the cell cytoplasm, i.e. 3- to 4-fold lower than in water. This is surprising, given the large concentration of solutes in the mitochondrion, and may indicate that matrix enzymes are present as membrane-associated complexes, leaving an unobstructed aqueous space that permits free diffusion of solutes. Using simulations, Olveczky and Verkman (1998) demonstrated that the presence of obstructions in the mitochondrion or the presence of a reticular system in the ER generally do not have a large effect on the diffusion of molecules in the lumen of these structures. However, Dayel et al. (1999) found that the rate of diffusion of a GFP-KDEL fusion protein present in the ER lumen was 9- to 18-fold lower than that in water, indicating the diffusion of some proteins in this compartment may be considerably slower than in other compartments. More recent studies suggest the presence of branched oligosaccharides on lumenal ER proteins or the interactions of ER proteins with chaperones may affect diffusion in the ER lumen (Nehls et al. 2000).

Using FITC-dextrans, Seksek et al. (1997) reported that, as in the cytoplasm, rates of macromolecular diffusion in the nucleus are 3- to 4-fold lower than in water. However, FRAP studies of GFP-fusion proteins using a number of proteins that localize in the nucleus show that these chimeras diffuse at rate up to 100-fold slower than in aqueous buffers (Kruhlak et al. 2000; Phair and Misteli 2000; Houtsmuller and Vermeulen 2000). As detailed below, this reflects the dynamic exchange between the proteins located in the nucleoplasm and those associated with specific nuclear compartments.

## Protein-protein associations

FRAP studies have been employed to demonstrate associations between proteins. Although the magnitude of the diffusion coefficient is only weakly sensitive to the

size of the diffusing species in membrane bilayers (Saffman and Delbruck 1975), protein aggregation or interactions of proteins with immobilized components can be readily monitored by FRAP analysis. Katzir et al. (1989) used FRAP to determine whether two proteins in the plasma membrane formed a complex. They employed antibodies to cross-link and immobilize one of the proteins and examined whether this had any affect on the diffusive properties of the other membrane protein. Knowles et al. (1994) reported that binding either a monoclonal antibody or its monovalent Fab fragment to the exoplasmic domain of glycophorin A in human erythrocytes immobilized the receptor, suggesting a co-operative coupling between liganded glycophorin A and the underlying membrane skeleton. Sloan-Lancaster et al. (1998) examined the interaction between ZAP-70 and T-cell receptor subunits on the plasma membrane by comparing the kinetics of recovery. The different kinetics of the two proteins and the ability to model the latter ($D \approx 0.01$ μm$^2$/s) but not the former ($D \approx 0.2$ μm$^2$/s) as simple diffusion within a membrane indicated the interaction between the two proteins was dynamic and that exchange with a cytoplasmic pool contributed to the recovery of the former. Ochoa et al. (2000) demonstrated an interaction between actin and dynamin in podosomes using GFP fusions. Both proteins gave rise to similar recovery kinetics following bleaching, thereby indicating their association.

Berk et al. (1997) used FRAP to quantitate the binding of a fluorescently labelled monoclonal antibody to cells. In the absence of binding, a rapid recovery was observed owing to aqueous diffusion of unbound antibody. In the presence of binding the fluorescence recovery was dependent on the diffusion of the cellular components and an analysis of the kinetic parameters allowed an estimation of the binding constant. The combination of FRAP with total internal reflection microscopy has also been widely employed to obtain such information (Thompson and Lagerholm 1997).

## FLIP for determining connectivity between compartments

The technique termed fluorescence loss in photobleaching (FLIP) has been used to reveal the connectivity between different compartments in the cell (Cole et al. 1996; Ellenberg et al. 1997). This involves repeatedly bleaching a small region in the cell and acquiring an image of the whole cell. The fluorescence from any regions that are connected to the bleached region will eventually disappear. By contrast, the fluorescence in unconnected regions will not be affected. This method has been used to illustrate the connectivity between some plastids in plant cells (Kohler et al. 1997), the continuity of the ER during various stages of the cell cycle (Ellenberg et al. 1997; Szczesna-Skorupa et al. 1998; Dayel et al. 1999; Kline et al. 1999; Terasaki 2000), the redistribution of Golgi contents to a continuous ER during mitosis (Zaal et al. 1999) and the presence of an open lumenal structure between the ER and the nuclear envelope (Subramanian and Meyer 1997). The technique has also been used to study the continuity between the ER membrane and the Golgi and nuclear membranes (Ostlund et al. 1999) and between the nucleus and cytoplasm (Sloan-Lancaster et al. 1998) and to reveal the fragmentation of the ER in presence of high calcium (Subramanian and Meyer 1997).

The FLIP technique can also be used to observe fluorescence from unconnected compartments that normally cannot be seen against the large fluorescence signal arising from other parts of the cell. For example, Dayel et al. (1999) found some residual polynuclear, Golgi-like fluorescence in CHO cells expressing GFP-KDEL after they had used FLIP to completely bleach the ER fluorescence. Nehls et al. (2000) used FLIP of the KDEL receptor in the ER to demonstrate that some of the receptor was located in post-ER compartments, which were not connected to the rest of the ER. Nakata et al. (1998) examined vesicular transport in axons by completely bleaching the fluorescence in an axonal region to permit visualization of the transport of weakly fluorescent transport vesicles.

## Image analysis for semi-quantitative determination of diffusion coefficients

The image profiles following bleaching and the time taken to achieve a certain degree of bleaching can provide qualitative information about the diffusion coefficients. For example, Fig. 4a shows bleaching of an erythrocyte labelled at the membrane skeleton with rhodamine-phalloidin. The image following a 0.1 s bleach shows localized loss of fluorescence in the bleached region. This

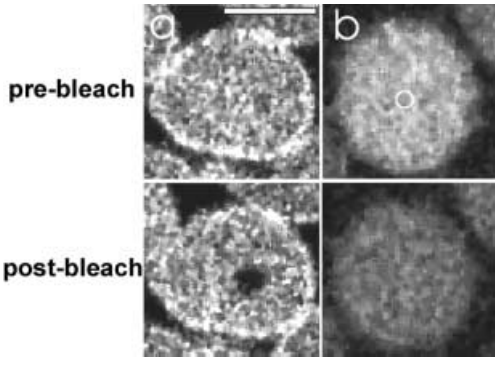


**Fig. 4a, b** Photobleaching of fluorescently labelled components in the human erythrocyte. **a** The erythrocyte cytoskeleton was labelled by incorporating rhodamine-phalloidin (which binds to actin) inside reversibly lysed erythrocytes. Images were obtained before and immediately after bleaching a region in the centre of the cell for 0.1 s. **b** CF-casein was incorporated into the cytosol of resealed erythrocytes. Images were obtained before and immediately after bleaching the indicated region for 0.1 s. Confocal images were obtained under the following conditions: pinhole 1.0 optical units, 512×512 pixels, 0.098 nm/pixel, 1.1 s/image. *Bar* = 5 μm

result, coupled with the absence of recovery (data not shown), is consistent with an immobile membrane skeleton. This contrasts with the bleaching of an erythrocyte containing carboxyfluorescein (CF)-casein in the cytosol (Fig. 4b). In this case, the image obtained following a 0.1 s bleach shows an even loss of fluorescence throughout the entire compartment. This is consistent with the rapid diffusion of CF-casein ($D \approx 50$ μm$^2$/s) within the confines of the cytosol, which has a cross-sectional surface area of about 30 μm$^2$. Hence, the time for image acquisition (~1 s) is sufficient for the CF-casein to equilibrate throughout the cytosol. In addition, the bleach time (0.1 s) was sufficient for a significant proportion of the CF-casein molecules to find themselves in the path of the bleaching beam, thereby producing the large loss of fluorescence throughout the cell.

A similar result is obtained with malaria parasite-infected erythrocytes expressing a GFP-fusion protein in the cytosol [Fig. 5a; see Wickham et al. (2001) for experimental details]. In this case a 5 s bleach results in the loss of fluorescence throughout the compartment, consistent with the GFP-fusion protein being present in a soluble form in the cytoplasm. Similar results have been reported with other GFP fusions located in the nucleus and cytoplasm of other cells (Sloan-Lancaster et al. 1998; Kruhlak et al. 2000).

A different bleach profile is observed when the GFP-fusion protein is located within the lumen of the parasitophorous vacuole (PV) that encloses the malaria parasite within the erythrocyte cytosol (see fig. 5E–H in Wickham et al. 2001). In this case, bleaching results in a loss of fluorescence throughout the entire PV but the loss is greatest in the region that is bleached. After 30 s, recovery of fluorescence into the bleached area was observed resulting in an even (though lower) fluorescence signal throughout the compartment. This result indicates that the lumen of the PV is continuous but that the diffusion of the GFP fusion is restricted compared to that in solution, possessing a recovery time on the order of seconds. Hence this result indicates that either (1) the viscosity within the PV is very large, (2) the lumen is highly constricted on the order of dimensions of the GFP-fusion molecule, (3) the GFP is in a highly aggregated form in the lumen or (4) the GFP-fusion protein is associated in some way with the membrane.

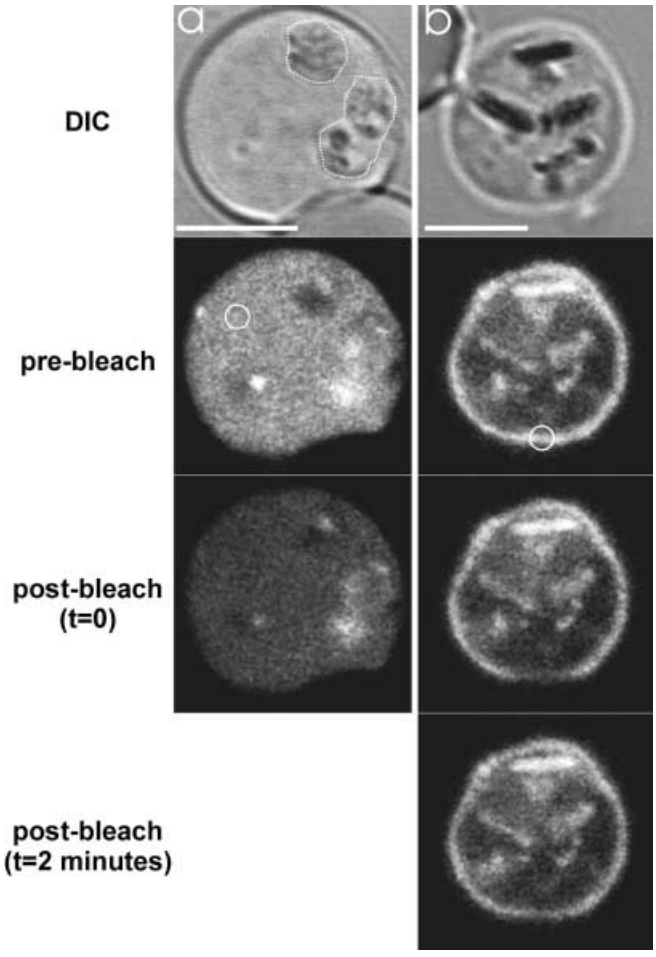


**Fig. 5a, b** Bleaching of GFP-fusion proteins in malaria parasite-infected erythrocytes. **a** An immature parasite-infected erythrocyte expressing a GFP-fusion protein in the erythrocyte cytosol. The DIC image shows ring stage parasites (*highlighted*) within the erythrocyte cytosol. The cell was bleached at the position indicated in the pre-bleach image for 5 s and the post-bleach image was obtained immediately after bleaching. **b** A mature parasite-infected erythrocyte expressing a GFP-fusion protein that is associated with the erythrocyte membrane. The DIC image shows a late-stage parasite in the erythrocyte cytosol. The pre-bleach image indicates that the fluorescent protein is associated with the erythrocyte membrane. The region indicated was bleached for 1 s and a post-bleach image obtained immediately and 2 min after bleaching. Confocal images were obtained under the following conditions: pinhole 1.0 optical unit, 512×512 pixels, 0.049 nm/pixel. Each image is the average of four consecutive images obtained at 1.1 s/image. *Bar* = 5 μm

## Dynamics of cellular components with bound and free forms

Many biological molecules are present in an equilibrium between bound and free states. For example, cytochrome *c* is a soluble protein located in the intermembrane space of mitochondria but also associates with the inner mitochondrial membrane. Hence, recovery of the fluorescence signal following photobleaching of the membrane-associated population occurs both from lateral diffusion within the membrane and by exchange with the free population (Gupte et al. 1984; Gupte and Hackenbrock 1988). Such instances can be identified in a number of ways:

(i) Estimation of the magnitude of the diffusion coefficient. Kwon et al. (1994) concluded that the large diffusion coefficient of the membrane-bound α-subunit of the G-protein (0.2 μm$^2$/s) reflected exchange with a cytoplasmic pool rather than lateral diffusion in the membrane. Luxon and Weisiger (1993) found that the low diffusion coefficient of a fluorescent fatty acid in the cytoplasm of rat hepatocytes (0.3–0.5 μm$^2$/s) reflected its association with fatty acid-binding proteins in the cytoplasm and with the cellular membrane.

(ii) Determination of the dependence of the measured diffusion coefficient on $\omega$ (Eq. 3; Henis et al. 1988). The GFP-Ras fusion protein, which is located predominantly in the plasma membrane, exhibits recovery kinetics that are dependent on the size of the beam, indicating that recovery is due to lateral diffusion (Niv et al. 1999). By contrast, the actin population present in stress fibres and focal contacts in embryonic chicken gizzard cells exhibits a slow recovery that is independent of bleach dimensions, indicating that recovery occurs via an exchange with diffusible cytosolic actin (Kreis et al. 1982).

(iii) Use of FLIP analysis to demonstrate that bleaching of one compartment affects another compartment. Vasudevan et al. (1998) found two populations of ADP-ribosylation factors that were located in the cytoplasm and associated with the Golgi, respectively. Bleaching of the cytoplasmic pool resulted in a decrease in fluorescence from the Golgi, demonstrating that the two populations were exchanging dynamically. Kruhlak et al. (2000) and Phair and Misteli (2000) have shown that nuclear-located proteins are present throughout the nucleoplasm but are concentrated in a number of nuclear compartments such as nucleoli and nucleosomes. During a FLIP experiment, loss of fluorescence associated with both foci and nucleoplasm in regions distal from the bleach spot occurred at similar rates, demonstrating that the proteins in the nucleoplasm and in the foci were in a dynamic equilibrium. Daigle et al. (2001) used FLIP analysis to show that the cytoplasmic and nuclear pools of the nuclear pore complex component, Nup153, exist as separate pools. Thus the fluorescence recovery observed following the bleaching of Nup153 associated with the nuclear pore complex was attributed to the presence of a soluble pool of the complex located in the nucleus and distinct from the cytoplasmic pool.

(iv) Examination of the spatial distribution of the recovery profile. Figure 2 shows that the spatial distribution of recovery due to lateral diffusion is complex and occurs at different rates in different regions of the bleached area. In contrast, recovery due to exchange with the aqueous phase results in all parts of the bleached area recovering at a similar rate. An examination of the spatial distribution of recovery can therefore provide a qualitative indication as to whether recovery is due to lateral diffusion or due to aqueous exchange. For example, Cuppen et al. (1999) found that the recovery of the fluorescence signal for a protein located in the submembrane region occurred evenly throughout the bleached area, indicating that recovery occurred through the exchange with a cytoplasmic pool. Similarly, Vikstrom et al. (1992) showed that the recovery of fluorescence from bleached vimentin intermediate filaments exhibits no polarity, indicating steady-state exchange of vimentin subunits along the length of the intermediate filament. Another example is illustrated in Fig. 5b, which shows a GFP-fusion protein expressed in a malaria parasite-infected erythrocyte that is trafficked to and associates with the cytoplasmic surface of the erythrocyte membrane (see Wickham et al. 2001 for details). In this case, bleaching the membrane region results in a localized loss of fluorescence in the region of the bleach. The bleached area exhibits some recovery after two minutes that could be due to diffusion of a membrane-embedded fluorescent protein into the bleached area. However, a quantitative analysis (not shown) shows that recovery occurs evenly throughout the bleached region, which suggests that the recovery of fluorescence probably occurs due to dissociation of bound bleached GFP-fusion proteins from the cytoskeletal network and binding of unbleached molecules from the aqueous pool onto this region. Independent evidence also suggests that the GFP-chimera is associated with components of the immobilized erythrocyte cytoskeleton rather than with an integral membrane protein (Wickham et al. 2001).

## Transport between compartments

The ability to selectively bleach specific compartments permits the quantitation of the transport of molecules across membranes or between subcellular compartments. Peters (1985) bleached the cytoplasmic contents of a cell and then analysed the recovery due to transport/diffusion of fluorescent solutes from the external medium to obtain quantitative information about transport across the plasma membrane. A similar technique has been employed to examine the level of communication between cells connected by gap junctions. In this case, cells were loaded with a fluorescent solute and the contents of one cell were bleached. The fluorescence recovered due to diffusion or transport of the solute through the gap junction connecting the cells (Wade et al. 1986; Pluciennik et al. 1996). In another variant of the technique, calcium-dependent transport of calmodulin between the cytoplasm and the nucleus was investigated by selectively bleaching the nuclear region and monitoring the recovery of fluorescence due to diffusion of calmodulin from the cytoplasm (Liao et al. 1999; Teruel et al. 2000).

## ''Bleach-chase'' experiments

Photobleaching measurements can be performed in a fashion analogous to the classical pulse chase experiments that utilize radiolabelled tracers, with the bleaching event employed to generate an instantaneous perturbation of the system that can be followed in real time. The fate of the bleached region and its effect on the rest of the cell can be examined to reveal various aspects of cellular dynamics. This approach has been used to examine the dynamics of the cytoskeleton (Okabe and Hirokawa 1990; Takeda et al. 1995; Yoon et al. 1998). For example, Okabe and Hirokawa (1990) found that bleached regions of fluorescently labelled actin filaments

and tubulin microtubules in murine neuronal axons did not move or spread down the axon but remained stationary and gradually recovered their fluorescence. These data indicated that microtubules and actin filaments are not rigid polymers moving forward within the axon, but are dynamic structures that continue to assemble along the length of the axon.

"Bleach-chase" measurements have also been employed to study various aspects of protein trafficking. Zaal et al. (1999) examined GFP-fusion proteins targeted to the Golgi. They utilized the ability of the confocal microscope to selectively bleach an irregular shape within a 2D confocal section to selectively bleach a target organelle. They observed a temporal decrease in Golgi fluorescence following bleaching of the ER as well as a recovery of Golgi fluorescence following bleaching of the Golgi. This demonstrated that the GFP-fusion proteins were continually recycled through the ER during interphase. Dahm et al. (2001) obtained similar results with VIP36, which is involved in protein trafficking between the ER and Golgi. In this case, they employed 3D bleaching to ensure that the entire organelle was bleached. Other measurements have demonstrated the exchange of proteins between Golgi structures (Cole et al. 1996; Storrie et al. 1998). The precise mechanism of the exchange is unclear and may reflect trafficking via an ER intermediate or diffusion through interconnected Golgi stacks.

### Landmark or patterned bleaching

The presence of an AOTF in modern confocal microscopes and the flexibility of modern software and hardware permit the user to define and bleach a region of any shape or pattern. This has been ingeniously utilized by Daigle et al. (2001) to "mark" a featureless component and permit its tracking. For example, a striped bleach pattern was used to mark the lamin network underlying the nuclear envelope. An examination of the dynamics of the striped pattern revealed occasional transient movement of the network followed by regeneration of the original image, showing it as a dynamic but elastic structure. In another application, a spot bleach pattern on the same lamin network was employed to demonstrate that there was no net movement of the nuclear pore complex relative to the underlying lamin network.

## Summary

The technique of FRAP was developed two decades ago but has recently undergone something of a renaissance owing to the development of confocal microscope-based methods for performing photobleaching experiments and the introduction of GFP as a convenient and highly specific label of particular cellular components. In this work we have examined some of the advantages, disadvantages and potential pitfalls of performing photobleaching studies using the confocal microscope. Innovative applications of the technique have enabled real-time analysis of the complex organization and reorganization of cellular components. Clearly, the potential uses of this very accessible technology are enormous.

**Acknowledgements** This work was supported by the Co-operative Research Centre for Diagnostics, Australia, and the National Health and Medical Research Council of Australia.

## References

Aizenbud BM, Gershon ND (1982) Diffusion of molecules on biological membranes of nonplanar form. A theoretical study. Biophys J 38:287–293

Angelides KJ, Elmer LW, Loftus D, Elson E (1988) Distribution and lateral mobility of voltage-dependent sodium channels in neurons. J Cell Biol 106:1911–1925

Arrio-Dupont M, Foucault G, Vacher M, Devaux PF, Cribier S (2000) Translational diffusion of globular proteins in the cytoplasm of cultured muscle cells. Biophys J 78:901–907

Axelrod D (1977) Cell surface heating during fluorescence photobleaching recovery experiments. Biophys J 18:129–131

Axelrod D (1983) Lateral motion of membrane proteins and biological function. J Membr Biol 75:1–10

Axelrod D, Koppel DE, Schlessinger J, Elson E, Webb WW (1976) Mobility measurement by analysis of fluorescence photobleaching recovery kinetics. Biophys J 16:1055–1069

Barisas BG, Leuther MD (1979) Fluorescence photobleaching recovery measurement of protein absolute diffusion constants. Biophys Chem 10:221–229

Berk DA, Yuan F, Leunig M, Jain RK (1993) Fluorescence photobleaching with spatial Fourier analysis: measurement of diffusion in light-scattering media. Biophys J 65:2428–2436

Berk DA, Yuan FL, Leunig M, Jain RK (1997) Direct in vivo measurement of targeted binding in a human tumor xenograft. Proc Natl Acad Sci USA 94:1785–1790

Blonk JCG, Don A, Aalst H van, Birmingham JJ (1993) Fluorescence photobleaching recovery in the confocal scanning light microscope. J Microsc 169:363–374

Bloom JA, Webb WW (1984) Photodamage to intact erythrocyte membranes at high laser intensities: methods of assay and suppression. J Histochem Cytochem 32:608–616

Brass JM, Higgins CF, Foley M, Rugman PA, Birmingham J, Garland PB (1986) Lateral diffusion of proteins in the periplasm of *Escherichia coli*. J Bacteriol 165:787–795

Brown EB, Wu ES, Zipfel W, Webb WW (1999) Measurement of molecular diffusion in solution by multiphoton fluorescence photobleaching recovery. Biophys J 77:2837–2849

Cardullo RA, Mungovan RM, Wolf DE (1991) Imaging membrane organization and dynamics. In: Dewey TG (ed) Biophysical and biochemical aspects of fluorescence spectroscopy. Plenum Press, New York, pp 231–260

Cherry RJ, Smith PR, Morrison IEG, Fernandez N (1998) Mobility of cell surface receptors: a re-evaluation. FEBS Lett 430:88–91

Cole NB, Smith CL, Sciaky N, Terasaki M, Edidin M, Lippincott-Schwartz J (1996) Diffusional mobility of Golgi proteins in membranes of living cells. Science 273:797–801

Cone RA (1972) Rotational diffusion of rhodopsin in the visual receptor membrane. Nat New Biol 236:39–43

Corbett JD, Cho MR, Golan DE (1994) Deoxygenation affects fluorescence photobleaching recovery measurements of red cell membrane protein lateral mobility. Biophys J 66:25–30

Cowan AE, Nakhimovsky L, Myles DG, Koppel DE (1997) Barriers to diffusion of plasma membrane proteins form early during guinea pig spermiogenesis. Biophys J 73:507–516

Cuppen E, Wijers M, Schepens J, Fransen J, Wieringa B, Hendriks W (1999) A FERM domain governs apical confinement of PTP-BL in epithelial cells. J Cell Sci 112:3299–3308

Dahm T, White J, Grill S, Fullekrug J, Stelzer EH (2001) Quantitative ER↔Golgi transport kinetics and protein separation upon Golgi exit revealed by vesicular integral membrane protein 36 dynamics in live cells. Mol Biol Cell 12:1481–1498

Daigle N, Beaudouin J, Hartnell L, Imreh G, Hallberg E, Lippincott-Schwartz J, Ellenberg J (2001) Nuclear pore complexes form immobile networks and have a very low turnover in live mammalian cells. J Cell Biol 154:71–84

Dayel MJ, Hom EF, Verkman AS (1999) Diffusion of green fluorescent protein in the aqueous-phase lumen of endoplasmic reticulum. Biophys J 76:2843–2851

Dundr M, Misteli T, Olson MO (2000) The dynamics of postmitotic reassembly of the nucleolus. J Cell Biol 150:433–446

Edidin M, Zuniga MC, Sheetz MP (1994) Truncation mutants define and locate cytoplasmic barriers to lateral mobility of membrane glycoproteins. Proc Natl Acad Sci USA 91:3378–3382

Ellenberg J, Siggia ED, Moreira JE, Smith CL, Presley JF, Worman HJ, Lippincott-Schwartz J (1997) Nuclear membrane dynamics and reassembly in living cells: targeting of an inner nuclear membrane protein in interphase and mitosis. J Cell Biol 138:1193–206

Elson EL (1985) Fluorescence correlation spectroscopy and photobleaching recovery. Annu Rev Phys Chem 36:379–406

Feder TJ, Brust-Mascher I, Slattery JP, Baird B, Webb WW (1996) Constrained diffusion or immobile fraction on cell surfaces: a new interpretation. Biophys J 70:2767–2773

Gribbon P, Hardingham TE (1998) Macromolecular diffusion of biological polymers measured by confocal fluorescence recovery after photobleaching. Biophys J 75:1032–1039

Gupte SS, Hackenbrock CR (1988) Multidimensional diffusion modes and collision frequencies of cytochrome *c* with its redox partners. J Biol Chem 263:5241–5247

Gupte S, Wu ES, Hoechli L, Hoechli M, Jacobson K, Sowers AE, Hackenbrock CR (1984) Relationship between lateral diffusion, collision frequency and electron transfer of mitochondrial inner membrane oxidation-reduction components. Proc Natl Acad Sci USA 81:2606–2610

Henis YI, Yaron T, Lamed R, Rishpon J, Sahar E, Katchalski-Katzir E (1988) Mobility of enzymes on insoluble substrates: the beta-amylase-starch gel system. Biopolymers 27:123–138

Houtsmuller AB, Vermeulen W (2000) Macromolecular dynamics in living cell nuclei revealed by fluorescence redistribution after photobleaching. Histochem Cell Biol 115:13–21

Ishihara A, Hou Y, Jacobson K (1987) The Thy-1 antigen exhibits rapid lateral diffusion in the plasma membrane of rodent lymphoid cells and fibroblasts. Proc Natl Acad Sci USA 84:1290–1293

Jacobson K, Wojcieszyn J (1984) The translational mobility of substances within the cytoplasmic matrix. Proc Natl Acad Sci USA 81:6747–6751

Jacobson K, Ishihara A, Inman R (1987) Lateral diffusion of proteins in membranes. Annu Rev Physiol 49 163–175

Jacobson K, Sheets ED, Simson R (1995) Revisiting the fluid mosaic model of membranes. Science 268:1441–1442

Jovin TM, Vaz WL (1989) Rotational and translational diffusion in membranes measured by fluorescence and phosphorescence methods. Methods Enzymol 172:471–513

Kao HP, Verkman AS (1996) Construction and performance of a photobleaching recovery apparatus with microsecond time resolution. Biophys Chem 59:203–210

Kao HP, Abney JR, Verkman AS (1993) Determinants of the translational mobility of a small solute in cell cytoplasm. J Cell Biol 120:175–184

Katzir Z, Gutman O, Henis YI (1989) Application of fluorescence photobleaching recovery to assess complex formation between the two envelope proteins of Sendai virus in membranes of fused human erythrocytes. Biochemistry 28:6400–6405

Kline D, Mehlmann L, Fox C, Terasaki M (1999) The cortical endoplasmic reticulum (ER) of the mouse egg: localization of ER clusters in relation to the generation of repetitive calcium waves. Dev Biol 215:431–442

Knowles DW, Chasis JA, Evans EA, Mohandas N (1994) Cooperative action between band 3 and glycophorin A in human erythrocytes: immobilization of band 3 induced by antibodies to glycophorin A. Biophys J 66:1726–1732

Knowles DW, Tilley L, Mohandas N, Chasis JA (1997) Erythrocyte membrane vesiculation: model for the molecular mechanism of protein sorting. Proc Natl Acad Sci USA 94:12969–12974

Kohler RH, Cao J, Zipfel WR, Webb WW, Hanson MR (1997) Exchange of protein molecules through connections between higher plant plastids. Science 276:2039–2042

Koppel DE (1979) Fluorescence redistribution after photobleaching. A new multipoint analysis of membrane translational dynamics. Biophys J 28:281–291

Kreis TE, Geiger B, Schlessinger J (1982) Mobility of microinjected rhodamine actin within living chicken gizzard cells determined by fluorescence photobleaching recovery. Cell 29:835–845

Kruhlak MJ, Lever MA, Fischle W, Verdin E, Bazett-Jones DP, Hendzel MJ (2000) Reduced mobility of the alternate splicing factor (ASF) through the nucleoplasm and steady state speckle compartments. J Cell Biol 150:41–51

Kubitscheck U, Wedekind P, Peters R (1994) Lateral diffusion measurement at high spatial resolution by scanning microphotolysis in a confocal microscope. Biophys J 67:948–956

Kwon G, Axelrod D, Neubig RR (1994) Lateral mobility of tetramethylrhodamine (TMR) labelled G protein alpha and beta gamma subunits in NG 108-15 cells. Cell Signal 6:663–679

Lepock JR, Thompson JE, Kruuv J, Wallach DFH (1978) Photoinduced crosslinking of membrane proteins by fluorescein isothiocyanate. Biochem Biophys Res Commun 85:344–350

Liao B, Paschal BM, Luby-Phelps K (1999) Mechanism of $Ca^{2+}$-dependent nuclear accumulation of calmodulin. Proc Natl Acad Sci USA 96:6217–6222

Lippincott-Schwartz J, Roberts TH, Hirschberg K (2000) Secretory protein trafficking and organelle dynamics in living cells. Annu Rev Cell Dev Biol 16:557–589

Luby-Phelps K, Taylor DL, Lanni F (1986) Probing the structure of cytoplasm. J Cell Biol 102:2015–2022

Luby-Phelps K, Castle PE, Taylor DL, Lanni F (1987) Hindered diffusion of inert tracer particles in the cytoplasm of mouse 3T3 cells. Proc Natl Acad Sci USA 84:4910–4913

Luby-Phelps K, Hori M, Phelps JM, Won D (1995) $Ca^{2+}$-regulated dynamic compartmentalization of calmodulin in living smooth muscle cells. J Biol Chem 270:21532–21538

Luxon BA, Weisiger RA (1993) Sex differences in intracellular fatty acid transport: role of cytoplasmic binding proteins. Am J Physiol 265:G831–G841

McCown JT, Evans E, Diehl S, Wiles HC (1981) Degree of hydration and lateral diffusion in phospholipid multibilayers. Biochemistry 20:3134–3138

Meyvis TK, De Smedt SC, Van Oostveldt P, Demeester J (1999) Fluorescence recovery after photobleaching: a versatile tool for mobility and interaction measurements in pharmaceutical research. Pharm Res 16:1153–1162

Mozo-Villarias A, Ware BR (1985) Actin oligomers below the critical concentration detected by fluorescence photobleaching recovery. Biochemistry 24:1544–1548

Nakata T, Terada S, Hirokawa N (1998) Visualization of the dynamics of synaptic vesicle and plasma membrane proteins in living axons. J Cell Biol 140:659–674

Nehls S, Snapp EL, Cole NB, Zaal KJ, Kenworthy AK, Roberts TH, Ellenberg J, Presley JF, Siggia E, Lippincott-Schwartz J (2000) Dynamics and retention of misfolded proteins in native ER membranes. Nat Cell Biol 2:E105–E106

Niv H, Gutman O, Henis YI, Kloog Y (1999) Membrane interactions of a constitutively active GFP-Ki-Ras 4B and their role in signaling. Evidence from lateral mobility studies. J Biol Chem 274:1606–1613

Ochoa GC, Slepnev VI, Neff L, Ringstad N, Takei K, Daniell L, Kim W, Cao H, McNiven M, Baron R, De Camilli P (2000) A

functional link between dynamin and the actin cytoskeleton at podosomes. J Cell Biol 150:377–389
Okabe S, Hirokawa N (1990) Turnover of fluorescently labelled tubulin and actin in the axon. Nature 343:479–482
Olveczky BP, Verkman AS (1998) Monte Carlo analysis of obstructed diffusion in three dimensions: application to molecular diffusion in organelles. Biophys J 74:2722–2730
Ostlund C, Ellenberg J, Hallberg E, Lippincott-Schwartz J, Worman HJ (1999) Intracellular trafficking of emerin, the Emery-Dreifuss muscular dystrophy protein. J Cell Sci 112:1709–1719
Partikian A, Olveczky B, Swaminathan R, Li Y, Verkman AS (1998) Rapid diffusion of green fluorescent protein in the mitochondrial matrix. J Cell Biol 140:821–829
Patterson GH, Knobel SM, Sharif WD, Kain SR, Piston DW (1997) Use of the green fluorescent protein and its mutants in quantitative fluorescence microscopy. Biophys J 73:2782–2790
Periasamy N, Verkman AS (1998) Analysis of fluorophore diffusion by continuous distributions of diffusion coefficients: application to photobleaching measurements of multicomponent and anomalous diffusion. Biophys J 75:557–567
Periasamy N, Bicknese S, Verkman AS (1996) Reversible photobleaching of fluorescein conjugates in air-saturated viscous solutions: singlet and triplet state quenching by tryptophan. Photochem Photobiol 63:265–271
Peters R (1983) Fluorescence microphotolysis. Diffusion measurements in single cells. Naturwissenschaften 70:294–302
Peters R (1985) Measurement of membrane transport in single cells by fluorescence microphotolysis. Trends Biochem Sci 10:223–227
Peters R, Cherry RJ (1982) Lateral and rotational diffusion of bacteriorhodopsin in lipid bilayers: experimental test of the Saffman-Delbruck equations. Proc Natl Acad Sci USA 79: 4317–4321
Peters R, Bruenger A, Schulten K (1981) Continuous fluorescence microphotolysis: a sensitive method for study of diffusion processes in single cells. Proc Natl Acad Sci USA 78:962–966
Petersen NO, Elson EL (1986) Measurements of diffusion and chemical kinetics by fluorescence photobleaching recovery and fluorescence correlation spectroscopy. Methods Enzymol 130:454–484
Phair RD, Misteli T (2000) High mobility of proteins in the mammalian cell nucleus. Nature 404:604–609
Pluciennik F, Verrecchia F, Bastide B, Herve JC, Joffre M, Deleze J (1996) Reversible interruption of gap junctional communication by testosterone propionate in cultured Sertoli cells and cardiac myocytes. J Membr Biol 149:169–177
Poo M, Cone RA (1974) Lateral diffusion of rhodopsin in the photoreceptor membrane. Nature 247:438–441
Reits EA, Neefjes JJ (2001) From fixed to FRAP: measuring protein mobility and activity in living cells. Nat Cell Biol 3:E145–E147
Saffman PG, Delbruck M (1975) Brownian motion in biological membranes. Proc Natl Acad Sci USA 72 3111–3113
Salome L, Cazeils JL, Lopez A, Tocanne JF (1998) Characterization of membrane domains by FRAP experiments at variable observation areas. Eur Biophys J 27:391–402
Scalettar BA, Selvin PR, Axelrod D, Klein MP, Hearst JE (1990) A polarized photobleaching study of DNA reorientation in agarose gels. Biochemistry 29:4790–4798
Sciaky N, Presley J, Smith C, Zaal KJ, Cole N, Moreira JE, Terasaki M, Siggia E, Lippincott-Schwartz J (1997) Golgi tubule traffic and the effects of brefeldin A visualized in living cells. J Cell Biol 139:1137–1155
Seksek O, Biwersi J, Verkman AS (1997) Translational diffusion of macromolecule-sized solutes in cytoplasm and nucleus. J Cell Biol 138:131–142
Siggia ED, Lippincott-Schwartz J, Bekiranov S (2000) Diffusion in inhomogeneous media: theory and simulations applied to whole cell photobleach recovery. Biophys J 79:1761–1770
Sloan-Lancaster J, Presley J, Ellenberg J, Yamazaki T, Lippincott-Schwartz J, Samelson LE (1998) ZAP-70 association with T cell receptor zeta (TCRzeta): fluorescence imaging of dynamic changes upon cellular stimulation. J Cell Biol 143:613–624
Smith BA, McConnell HM (1978) Determination of molecular motion in membranes using periodic pattern photobleaching. Proc Natl Acad Sci USA 75:2759–2763
Smith LM, McConnell HM, Smith BA, Parce JW (1981) Pattern photobleaching of fluorescent lipid vesicles using polarized laser light. Biophys J 33:139–146
Soumpasis DM (1983) Theoretical analysis of fluorescence photobleaching recovery experiments. Biophys J 41:95–97
Stolpen AH, Brown CS, Golan DE (1988) Characterization of microscopic laser beams by 2-D scanning of fluorescence emission. Appl Opt 27:4414–4422
Storrie B, Kreis TE (1996) Probing the mobility of membrane proteins inside the cell. Trends Cell Biol 6:321–324
Storrie B, Pepperkok R, Stelzer EH, Kreis TE (1994) The intracellular mobility of a viral membrane glycoprotein measured by confocal microscope fluorescence recovery after photobleaching. J Cell Sci 107:1309–1319
Storrie B, White J, Rottger S, Stelzer EH, Suganuma T, Nilsson T (1998) Recycling of Golgi-resident glycosyltransferases through the ER reveals a novel pathway and provides an explanation for nocodazole-induced Golgi scattering. J Cell Biol 143:1505–1521
Stout AL, Axelrod D (1995) Spontaneous recovery of fluorescence by photobleached surface-adsorbed proteins. Photochem Photobiol 62:239–244
Subramanian K, Meyer T (1997) Calcium-induced restructuring of nuclear envelope and endoplasmic reticulum calcium stores. Cell 89:963–971
Swaminathan R, Bicknese S, Periasamy N, Verkman AS (1996) Cytoplasmic viscosity near the cell plasma membrane: translational diffusion of a small fluorescent solute measured by total internal reflection-fluorescence photobleaching recovery. Biophys J 71:1140–1151
Swaminathan R, Hoang CP, Verkman AS (1997) Photobleaching recovery and anisotropy decay of green fluorescent protein GFP-S65T in solution and cells: cytoplasmic viscosity probed by green fluorescent protein translational and rotational diffusion. Biophys J 72:1900–1907
Szczesna-Skorupa E, Chen CD, Rogers S, Kemper B (1998) Mobility of cytochrome P450 in the endoplasmic reticulum membrane. Proc Natl Acad Sci USA 95:14793–14798
Takeda S, Funakoshi T, Hirokawa N (1995) Tubulin dynamics in neuronal axons of living zebrafish embryos. Neuron 14:1257–1264
Terasaki M (2000) Dynamics of the endoplasmic reticulum and golgi apparatus during early sea urchin development. Mol Biol Cell 11:897–914
Teruel MN, Chen W, Persechini A, Meyer T (2000) Differential codes for free Ca(2+)-calmodulin signals in nucleus and cytosol. Curr Biol 10:86–94
Thomas JL, Holowka D, Baird B, Webb WW (1994) Large-scale co-aggregation of fluorescent lipid probes with cell surface proteins. J Cell Biol 125:795–802
Thompson NL, Axelrod D (1980) Reduced lateral mobility of a fluorescent lipid probe in cholesterol-depleted erythrocyte membrane. Biochim Biophys Acta 597:155–165
Thompson NL, Lagerholm BC (1997) Total internal reflection fluorescence: applications in cellular biophysics. Curr Opin Biotechnol 8:58–64
Thompson NL, Pearce KH, Hsieh HV (1993) Total internal reflection fluorescence microscopy: application to substrate-supported planar membranes. Eur Biophys J 22:367–378
Tocanne JF, Dupou-Cezanne L, Lopez A, Tournier JF (1989) Lipid lateral diffusion and membrane organization. FEBS Lett 257:10–16
Tsay T-T, Jacobson KA (1991) Spatial Fourier analysis of video photobleaching measurements. Principles and optimization. Biophys J 60:360–368
Tsuji A, Ohnishi S (1986) Restriction of the lateral motion of band 3 in the erythrocyte membrane by the cytoskeletal network:

dependence on spectrin association state. Biochemistry 25:6133–6139
Vasudevan C, Han W, Tan Y, Nie Y, Li D, Shome K, Watkins SC, Levitan ES, Romero G (1998) The distribution and translocation of the G protein ADP-ribosylation factor 1 in live cells is determined by its GTPase activity. J Cell Sci 111:1277–1285
Vaz WL, Criado M, Madeira VM, Schoellmann G, Jovin TM (1982) Size dependence of the translational diffusion of large integral membrane proteins in liquid-crystalline phase lipid bilayers. A study using fluorescence recovery after photobleaching. Biochemistry 21:5608–5612
Vaz WL, Goodsaid-Zalduondo F, Jacobson K (1984) Lateral diffusion of lipids and proteins in bilayer membranes. FEBS Lett 174:199–207
Vaz WL, Clegg RM, Hallmann D (1985) Translational diffusion of lipids in liquid crystalline phase phosphatidylcholine multibilayers. A comparison of experiment with theory. Biochemistry 24:781–786
Velez M, Axelrod D (1988) Polarized fluorescence photobleaching recovery for measuring rotational diffusion in solutions and membranes. Biophys J 53:575–591
Vikstrom KL, Lim SS, Goldman RD, Borisy GG (1992) Steady state dynamics of intermediate filament networks. J Cell Biol 118:121–129
Wade MH, Trosko JE, Schindler M (1986) A fluorescence photobleaching assay of gap junction-mediated communication between human cells. Science 232:525–528
Webb WW (1981) Luminescence measurements of macromolecular mobility. Ann NY Acad Sci 366:300–314
Wedekind P, Kubitscheck U, Heinrich O, Peters R (1996) Line-scanning microphotolysis for diffraction-limited measurements of lateral diffusion. Biophys J 71:1621–1632
Wey C-L, Cone RA, Edidin MA (1981) Lateral diffusion of rhodopsin in photoreceptor cells measured by fluorescence photobleaching and recovery. Biophys J 33:225–232
White J, Stelzer E (1999) Photobleaching GFP reveals protein dynamics inside live cells. Trends Cell Biol 9:61–65
Wickham ME, Rug M, Ralph SA, Klonis N, McFadden GI, Tilley L, Cowman AF (2001) Trafficking and assembly of the cytoadherence complex in *Plasmodium falciparum*-infected human erythrocytes. EMBO J 20:5636–5649
Wojcieszyn JW, Schlegel RA, Wu E-S, Jacobson KA (1981) Diffusion of injected macromolecules within the cytoplasm of living cells. Proc Natl Acad Sci USA 78:4407–4410
Wolf DE (1992) Theory of fluorescence recovery after photobleaching measurements on cylindrical surfaces. Biophys J 61:487–493
Wolf DE, Henkart P, Webb WW (1980a) Diffusion, patching, and capping of stearoylated dextrans on 3T3 cell plasma membranes. Biochemistry 19:3893–3904
Wolf DE, Edidin M, Dragsten PR (1980b) Effect of bleaching light on measurements of lateral diffusion in cell membranes by the fluorescence photobleaching recovery method. Proc Natl Acad Sci USA 77:2043–2045
Wu E-S, Jacobson K, Szoka F, Portis A (1978) Lateral diffusion of a hydrophobic peptide, N4-nitrobenz-2-oxa-1,3-diazole gramicidin S, in phospholipid multibilayers. Biochemistry 17:5543–5550
Yechiel E, Edidin M (1987) Micrometer-scale domains in fibroblast plasma membranes. J Cell Biol 105:755–760
Yguerabide J, Schmidt JA, Yguerabide EE (1982) Lateral mobility in membranes as detected by fluorescence recovery after photobleaching. Biophys J 40:69–75
Yoon M, Moir RD, Prahlad V, Goldman RD (1998) Motile properties of vimentin intermediate filament networks in living cells. J Cell Biol 143:147–157
Zaal KJ, Smith CL, Polishchuk RS, Altan N, Cole NB, Ellenberg J, Hirschberg K, Presley JF, Roberts TH, Siggia E, Phair RD, Lippincott-Schwartz J (1999) Golgi membranes are absorbed into and reemerge from the ER during mitosis. Cell 99:589–601
Zoelen EJ van, Tertoolen LG, Laat SW de (1983) Simple computer method for evaluation of lateral diffusion coefficients from fluorescence photobleaching recovery kinetics. Biophys J 42:103–108
Zs.-Nagy I, Ohta, M, Kitani, K, Imahori K (1985) An automated method for measuring lateral mobility of proteins in the plasma membrane of cells in compact tissues by means of fluorescence recovery after photobleaching. Mikroskopie 41:12–25